

Accelerated 3D Imaging of Oxygen Partial Pressure using Projection Acquisition and Constrained Reconstruction

R. L. O'Halloran¹, J. H. Holmes¹, and S. B. Fain^{1,2}

¹Medical Physics, University of Wisconsin, Madison, WI, United States, ²Radiology, University of Wisconsin, Madison, WI, United States

Introduction: Hyperpolarized (HP) Helium-3 MRI has been shown to provide quantitative functional information such as diffusion coefficient [1] and partial pressure of oxygen (pO_2) [2]. Acquiring these parametric maps is challenging, however, because of finite polarization and short patient breath-hold times (~20 s). Undersampled projection imaging combined with constrained reconstruction methods has the potential to accelerate imaging and requires fewer RF pulses per image. The particular combination of 3D stack-of-stars and iterative highly constrained back-

Methods: MRI was performed with a 3D stack-of-stars fast-GRE sequence on a 1.5 T MR scanner (Signa Excite, GE Healthcare, Milwaukee, WI) with a chest coil tuned to the He-3 resonant frequency used to transmit and receive, ± 62.5 MHz bandwidth, 3 cm slice thickness, 128 readout points, and 256 projections acquired in a pseudo random order. The phantom was filled with 160 mL O_2 , 160 mL 3He , and 640 mL N_2 and imaged with 8 z phase encodings, TR/TE = 6.8/5.0 ms at a 35 cm FOV and 20 s scan time. The volunteer was imaged following inhalation of an anoxic 1 L mixture of 5 mMol hyperpolarized 3He with 10 z phase encodings, TR/TE = 2.2/0.7 ms at a 42 cm FOV and 16 s scan time. Imaging was conducted according to Fig 1, where each gray block represents 16 projections per phase encoding and the height of each block represents the flip angle used during the block. For the phantom scan $t_a=1.37$ s, $t_b=0.87$ s, and in the volunteer scan $t_a=1.35$ s, $t_b=0.35$ s.

Reconstruction: Each group of 16 consecutively acquired angles were reconstructed separately providing 16 time-frame images per slice. Iterative HYPR was performed on each of the 16 projection images with iteration terminated after a minimum squared difference between the measured and reconstructed data was reached. The constraining image was composed of all 256 projections.

Data Analysis: The last 5 images were fit to obtain a flip angle map used to correct the first 11 images. pO_2 maps were calculated from these first 11 images from scaled log ratios of each image to the first image in the time-series [2].

Results and Discussion: The pO_2 in the bag was plotted as a function of time (Fig 2a) and was in good agreement with the expected constant value of 0.16 bar. The pO_2 (Fig 2b) and flip angle maps (Fig 2c) exhibit some inhomogeneity which is most likely due to the non-uniform flip angle, combined with diffusion effects. Two consecutive slices of the volunteer scan are presented in Figure 3. The flip angle (Fig 3a and 3b) varies regionally from 2° in the posterior regions to 1.5° in the anterior regions with the region of highest flip angle differing between the two slices. In contrast, the pO_2 maps from the two slices are very similar, indicating that the observed regional differences in pO_2 are not merely due to errors in the flip angle fitting. Vertical profiles through the right lung for slices 4 (Fig 3e blue line) and 5 (Fig 3e red line) are displayed and both depict the expected gravity-induced dependence of pO_2 on anterior to posterior position [5].

Conclusion: A 3D stack-of-stars acquisition combined with I-HYPR reconstruction for pO_2 mapping was validated in a bag phantom and demonstrated in a healthy volunteer. Dependence of the pO_2 on Anterior/posterior position was observed in the volunteer. The technique provides 16 images of 10 slices at $3.2 \times 3.2 \times 30$ mm resolution in 16 seconds allowing for single acquisition pO_2 mapping. The acquisition was designed to maximize SNR in by modulating the flip-angle in later time-frames, however, the flip-angle scheme may be readily modified to be robust against lost patient breath-holds at the expense of image quality. Future work will focus on optimizing the acquisition and examining both healthy and diseased populations.

References: [1] 1st Diffusion paper. [2] Deninger et al. JMR (1999) [3] O'Halloran et al. MRM (in press) [4] O'Halloran et al ISMRM 2007. [5] Levitsky *Pulmonary Physiology* 6th Ed. McGraw Hill 2003

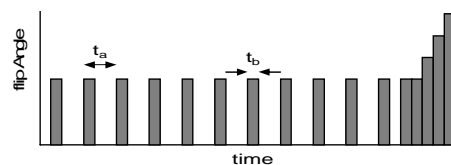


Figure 1: The acquisition incorporates variable flip and angle and delays between images to separate the oxygen and flip angle effects. t_a is the delay between images and t_b is the time to acquire an image.

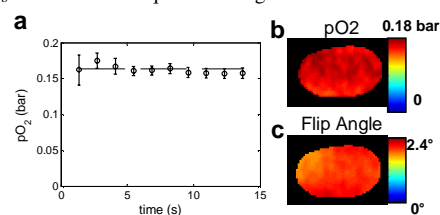


Figure 2: (a) The measured dependence of pO_2 on time in the phantom is constant at the expected value of 0.16 bar. (b) The pO_2 map exhibits inhomogeneity that is probably due to diffusion effects combined with a non-uniform flip angle (c).

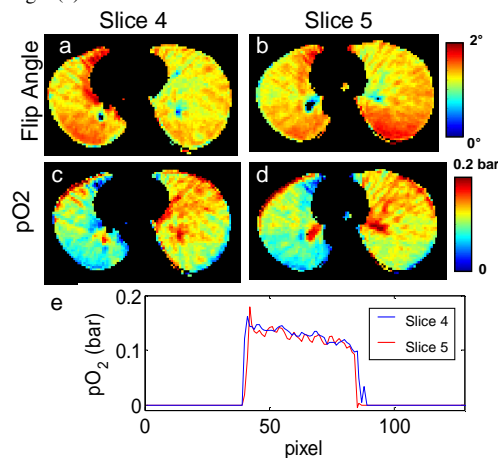


Figure 3: (a,b) The flip angle maps from two slices 12.9 s into the breath-hold and the corresponding pO_2 maps (c,d) from the same two slices. (e) Anterior/posterior profiles taken from the right lung 12 seconds into the scan show trend of decreasing pO_2 from anterior to posterior.